

Mixed convection flow in a vertical circular duct with time-periodic boundary conditions: steady-periodic regime

A. Barletta ^{*}, E. Rossi di Schio

Dipartimento di Ingegneria Energetica, Nucleare e del Controllo Ambientale (DIENCA), Laboratorio di Montecuccolino, Università di Bologna, Via dei Colli 16, I-40136 Bologna, Italy

Received 10 November 2003; received in revised form 9 February 2004
Available online 19 March 2004

Abstract

Mixed convection flow in a vertical circular duct subjected to a periodic sinusoidal temperature change at the wall is investigated. The analysis is performed by considering fully-developed parallel flow and steady-periodic regime. The local momentum and energy balance equations, together with the constraint equations which arise from the definition of mean velocity and mean temperature, are written in a dimensionless form and mapped into equations in the complex domain. One obtains two independent boundary value problems, which provide the mean value and the oscillating term of the velocity and temperature distributions. These boundary value problems are solved analytically, and the velocity and temperature distributions are obtained as functions of three parameters: the Prandtl number, Pr , the dimensionless frequency Ω , the ratio between the Grashof number Gr and the Reynolds number Re . The Fanning friction factor and the dimensionless heat flux are evaluated.

© 2004 Elsevier Ltd. All rights reserved.

Keywords: Laminar flow; Mixed convection; Circular duct; Analytical methods; Unsteady solutions

1. Introduction

Unsteady boundary conditions compatible with a steady-periodic regime have been widely studied with reference to forced convection flows [1–5]. On the contrary, the effects of buoyancy on steady-periodic flows are not so widely investigated. The interest deserved to this argument is mainly due to its technological applications, such as, for instance, the thermal control of electric resistors in alternating current or the development of heat-exchange enhancement techniques based on flows with time-oscillating mass rates.

In Refs. [6–9], natural convection is studied numerically in a two-dimensional rectangular cavity with two horizontal adiabatic walls, one vertical wall with uni-

form and constant temperature and the other vertical wall subjected either to a uniform temperature distribution which varies in time according to a sinusoidal law [6,7], or to a uniform heat flux distribution which undergoes a periodic square wave time-change [8,9]. In Refs. [7–9], the existence of a resonance phenomenon is predicted, namely the existence of a frequency of the wall thermal oscillations which corresponds to a maximum of the heat flux amplitude throughout any vertical surface in the cavity. Discrepant results have been found in Refs. [6,7] about the influence of the oscillation frequency on the time-averaged heat flux: this influence is considered as negligible in Ref. [6], while in Ref. [7] it is shown that, for wall temperature oscillations having a sufficiently high amplitude, there exists a critical frequency which corresponds to a maximum of the time-averaged heat flux. In Ref. [10], free convection is studied around a vertical plane subjected to a uniform and time-periodic temperature distribution. In Ref. [11], mixed convection in an inclined parallel-plate channel is investigated, with thermal boundary conditions such

^{*} Corresponding author. Tel.: +39-051-6441703; fax: +39-051-6441747.

E-mail addresses: antonio.barletta@unibo.it (A. Barletta), eugenia.rossidischio@unibo.it (E. Rossi di Schio).

Nomenclature

$A(t)$	function of time, defined in Eq. (7)	\mathbf{U}	fluid velocity
A_1, A_2	integration constants	U	X -component of the fluid velocity
f	Fanning friction factor, defined by Eq. (15)	U_0	mean fluid velocity in a duct section, defined by Eq. (3)
f_a^*, f_b^*	dimensionless complex valued functions, defined in Eq. (37)	W	wronskian
$F(s)$	function defined in Eq. (32)	X	axial coordinate
g	magnitude of the gravitational acceleration	<i>Greek symbols</i>	
G_1, G_2, G_3, G_4	Functions defined in Eq. (34)	α	thermal diffusivity
Gr	Grashof number, defined in Eq. (10)	β	volumetric coefficient of thermal expansion
i	imaginary unit	ΔT	amplitude of the wall temperature oscillations
I_n	modified Bessel function of first kind and order n	λ	dimensionless parameter, defined in Eq. (10)
K_n	modified Bessel function of second kind and order n	λ^*	dimensionless complex-valued function, defined in Eq. (19)
k	thermal conductivity	λ_a^*, λ_b^*	dimensionless complex-valued functions, defined in Eq. (21)
n	integer number	η	dimensionless parameter, defined in Eq. (10)
p	pressure	θ	dimensionless temperature, defined in Eq. (10)
P	difference between the pressure and the hydrostatic pressure	θ^*	dimensionless complex-valued function, defined in Eq. (19)
Pr	Prandtl number, defined in Eq. (10)	θ_a^*, θ_b^*	dimensionless complex-valued functions, defined in Eq. (21)
q	heat flux per unit area	μ	dynamic viscosity
R	radial coordinate	ν	kinematic viscosity
R_0	radius of the cylinder	Φ	dimensionless heat flux, defined in Eq. (40)
r	$= R/(2R_0)$ dimensionless radial coordinate	Φ_a^*, Φ_b^*	dimensionless complex-valued functions, defined in Eq. (41)
Re	Reynolds number, defined in Eq. (10)	ξ	dimensionless parameter, defined in Eq. (10)
$\Re e$	real part of a complex number	ϱ	mass density
s	complex number	ϱ_0	mass density for $T = T_0$
t	time	$\bar{\tau}_w$	average wall shear stress, defined by Eq. (29)
T	temperature	ω	frequency of the wall temperature oscillations, defined in Eq. (1)
T_0	mean temperature in a duct section, defined by Eq. (4)	Ω	dimensionless frequency, defined in Eq. (10)
T_1	mean wall temperature		
u	$= U/U_0$, dimensionless velocity		
u^*	dimensionless complex-valued function, defined in Eq. (19)		
u_a^*, u_b^*	dimensionless complex-valued functions, defined in Eq. (21)		

that one wall is kept at a constant temperature and the other is subjected to a sinusoidal temperature oscillation. The authors show that, for any value of the Prandtl number greater than 0.277, there exists a resonance frequency of the friction factor evaluated at the wall with an unsteady temperature. Moreover, for every plane which lies between the midplane of the channel and the wall subjected to the oscillating boundary condition, any value of the Prandtl number corresponds to a resonance frequency of the dimensionless heat flux.

The aim of the present paper is to investigate laminar mixed convection in the steady-periodic regime for a Newtonian fluid in a vertical circular duct. Reference is made to the fully developed region, and the thermal

boundary condition is given by a uniform wall temperature distribution which undergoes a sinusoidal time-change. The study is performed with analytical methods. In particular, the local momentum and energy balance equations, together with the boundary conditions and the constraint equations which arise from the definition of mean velocity and mean temperature, are written in a dimensionless form and mapped onto differential equations and constraint equations in the complex domain. A pair of independent boundary value problems is obtained, which provides both the mean value and the oscillating part of the temperature and velocity distributions. The pair of boundary value problems is solved analytically and the dimensionless distributions are ob-

tained as functions of three parameters: the Prandtl number Pr , the dimensionless angular frequency Ω , the ratio between the Grashof number Gr and the Reynolds number Re .

2. Governing equations

Let us consider a Newtonian fluid which steadily flows in a vertical duct with an infinite length and a circular cross section. The thermal conductivity k , the thermal diffusivity α and the dynamic viscosity μ of the fluid are treated as constants. Let X be the axial coordinate, chosen parallel to the gravitational acceleration \mathbf{g} but with opposite direction. Let us assume that the flow is laminar and parallel, so that only the X -component U of the velocity vector \mathbf{U} is nonzero. A parallel-velocity regime always exists in the case of fully developed flow inside a vertical duct, provided that the buoyancy forces are not too intense. In other words, a parallel-velocity regime for vertical mixed convection flows is stable for sufficiently small values of the Grashof number. For higher values of the Grashof number, multi-cell patterns arise, so that even in the fully developed region no parallel flow exists anymore.

The effect of viscous dissipation in the fluid is neglected and the Boussinesq approximation is employed. Since this approximation implies that the velocity field is solenoidal, one has $\partial U / \partial X = 0$, i.e. $U = U(R, t)$. Let us assume that the wall at $R = R_0$ is kept at an oscillating temperature, namely

$$T(X, R_0, t) = T_1 + \Delta T \cos(\omega t). \tag{1}$$

Moreover, since the thermal boundary condition (1) does not yield any net fluid heating or cooling, heat transfer occurs only in the radial direction, so that

$$\frac{\partial T}{\partial X} = 0, \tag{2}$$

i.e. $T = T(R, t)$. The prescribed mass flow rate is assumed to be stationary, so that the mean velocity in a duct cross section, defined as

$$U_0 = \frac{2}{R_0^2} \int_0^{R_0} dR U(R, t) R \tag{3}$$

is time-independent. Moreover, with reference to the Boussinesq approximation, let us choose the reference temperature as the average value of the fluid temperature with respect both to a duct cross section and to a period of time, namely

$$T_0 = \frac{\omega}{\pi R_0^2} \int_0^{2\pi/\omega} dt \int_0^{R_0} dR T(R, t) R. \tag{4}$$

Obviously, since $\partial T / \partial X = 0$, T_0 is a constant. On account of the above assumptions, the X -component and

the R -component of the momentum balance equation are

$$\varrho_0 \frac{\partial U}{\partial t} = - \frac{\partial P}{\partial X} + \varrho_0 g \beta (T - T_0) + \mu \nabla^2 U, \tag{5}$$

$$\frac{\partial P}{\partial R} = 0, \tag{6}$$

where $P = p + \varrho_0 g \beta$ is the difference between the pressure and the hydrostatic pressure. By differentiating both sides of Eq. (5) with respect to X , one obtains $\partial^2 P / \partial X^2 = 0$. This result implies the existence of a function $A(t)$ such that

$$\frac{\partial P}{\partial X} = -A(t). \tag{7}$$

Then, Eq. (5) can be rewritten as

$$\varrho_0 \frac{\partial U}{\partial t} = A(t) + \varrho_0 g \beta (T - T_0) + \frac{\mu}{R} \frac{\partial}{\partial R} \left(R \frac{\partial U}{\partial R} \right). \tag{8}$$

The energy balance equation is given by

$$\frac{\partial T}{\partial t} = \frac{\alpha}{R} \frac{\partial}{\partial R} \left(R \frac{\partial T}{\partial R} \right). \tag{9}$$

Let us define the following dimensionless variables:

$$\begin{aligned} \theta &= \frac{T - T_0}{\Delta T}, & r &= \frac{R}{2R_0}, & u &= \frac{U}{U_0}, & \eta &= \omega t, \\ \Omega &= \frac{4R_0^2 \omega}{\nu}, & \lambda &= \frac{4R_0^2 A(t)}{\mu U_0}, & Re &= \frac{2R_0 U_0}{\nu}, \\ Gr &= \frac{8g\beta\Delta TR_0^3}{\nu^2}, & \zeta &= \frac{T_1 - T_0}{\Delta T}, & Pr &= \frac{\nu}{\alpha}. \end{aligned} \tag{10}$$

Eqs. (8) and (9) can be rewritten in the following dimensionless form:

$$\Omega \frac{\partial u}{\partial \eta} = \lambda + \frac{Gr}{Re} \theta + \frac{1}{r} \frac{\partial}{\partial r} \left(r \frac{\partial u}{\partial r} \right), \tag{11}$$

$$\Omega Pr \frac{\partial \theta}{\partial \eta} = \frac{1}{r} \frac{\partial}{\partial r} \left(r \frac{\partial \theta}{\partial r} \right). \tag{12}$$

The boundary conditions for the dimensionless velocity distribution $u(r, \eta)$ and for the dimensionless temperature distribution $\theta(r, \eta)$ are as follows:

$$u(1/2, \eta) = 0, \quad \theta(1/2, \eta) = \zeta + \cos \eta. \tag{13}$$

Moreover, on account of Eqs. (3) and (4), one obtains two constraint equations for the dimensionless velocity and for the dimensionless temperature respectively, namely

$$\begin{aligned} \int_0^{1/2} dr u(r, \eta) r &= \frac{1}{8}, \\ \int_0^{2\pi} d\eta \int_0^{1/2} dr \theta(r, \eta) r &= 0. \end{aligned} \tag{14}$$

One can define the Fanning friction factor as

$$f = \frac{2\bar{\tau}_w}{\rho_0 U_0^2} = - \frac{2}{Re} \frac{\partial u}{\partial r} \Big|_{r=1/2}. \tag{15}$$

By differentiating with respect to η both sides of the integral constraint on $u(r, \eta)$ expressed in Eq. (14), one obtains

$$\int_0^{1/2} dr \frac{\partial u(r, \eta)}{\partial \eta} r = 0. \tag{16}$$

If one multiplies both sides of Eq. (11) by r and integrates with respect to r in the interval $[0, 1/2]$, one is led to the integral balance equation

$$\frac{\partial u}{\partial r} \Big|_{r=1/2} + \frac{\lambda}{4} + 2 \frac{Gr}{Re} \int_0^{1/2} dr \theta(r, \eta) r = 0. \tag{17}$$

It can be easily shown that, as a consequence of Eq. (17), the parameters f and λ are related through the expression

$$f Re = \frac{\lambda}{2} + 4 \frac{Gr}{Re} \int_0^{1/2} dr \theta(r, \eta) r. \tag{18}$$

3. Analytical solution: velocity and temperature distributions

In the steady periodic regime, one can solve analytically the momentum and energy balance equations (11), (12), together with the boundary conditions (13) and the constraints (14), by considering the functions $u(r, \eta)$, $\theta(r, \eta)$ and $\lambda(\eta)$ as the real parts of three complex valued functions, namely:

$$\begin{aligned} u(r, \eta) &= \Re e[u^*(r, \eta)], \\ \theta(r, \eta) &= \Re e[\theta^*(r, \eta)], \\ \lambda(\eta) &= \Re e[\lambda^*(\eta)]. \end{aligned} \tag{19}$$

On account of Eqs. (11)–(14), the complex valued functions $u^*(r, \eta)$, $\theta^*(r, \eta)$ and $\lambda^*(\eta)$ must be the solution of the following boundary value problem:

$$\begin{aligned} \Omega \frac{\partial u^*}{\partial \eta} &= \lambda^* + \frac{Gr}{Re} \theta^* + \frac{1}{r} \frac{\partial}{\partial r} \left(r \frac{\partial u^*}{\partial r} \right), \\ \Omega Pr \frac{\partial \theta^*}{\partial \eta} &= \frac{1}{r} \frac{\partial}{\partial r} \left(r \frac{\partial \theta^*}{\partial r} \right), \\ u^*(1/2, \eta) &= 0, \quad \theta^*(1/2, \eta) = \zeta + e^{i\eta}, \\ \int_0^{1/2} dr u^*(r, \eta) r &= \frac{1}{8}, \quad \int_0^{2\pi} d\eta \int_0^{1/2} dr \theta^*(r, \eta) r = 0. \end{aligned} \tag{20}$$

Therefore, one has

$$\begin{aligned} u^*(r, \eta) &= u_a^*(r) + \frac{Gr}{Re} u_b^*(r) e^{i\eta}, \\ \theta^*(r, \eta) &= \theta_a^*(r) + \theta_b^*(r) e^{i\eta}, \\ \lambda^*(\eta) &= \lambda_a^* + \frac{Gr}{Re} \lambda_b^* e^{i\eta}. \end{aligned} \tag{21}$$

By substituting Eq. (21) into Eq. (20), one obtains two independent boundary value problems. The first boundary value problem is expressed as

$$\begin{aligned} \frac{1}{r} \frac{d}{dr} \left(r \frac{du_a^*}{dr} \right) + \lambda_a^* + \frac{Gr}{Re} \theta_a^* &= 0, \\ \frac{d}{dr} \left(r \frac{d\theta_a^*}{dr} \right) &= 0, \\ u_a^*(1/2) = 0, \quad \theta_a^*(1/2) &= \zeta, \\ \int_0^{1/2} dr u_a^*(r) r &= \frac{1}{8}, \quad \int_0^{1/2} dr \theta_a^*(r) r = 0, \end{aligned} \tag{22}$$

while the second is given by

$$\begin{aligned} \frac{1}{r} \frac{d}{dr} \left(r \frac{du_b^*}{dr} \right) + \lambda_b^* + \theta_b^* &= i\Omega u_b^*, \\ \frac{1}{r} \frac{d}{dr} \left(r \frac{d\theta_b^*}{dr} \right) &= i\Omega Pr \theta_b^*, \\ u_b^*(1/2) = 0, \quad \theta_b^*(1/2) &= 1, \\ \int_0^{1/2} dr u_b^*(r) r &= 0. \end{aligned} \tag{23}$$

The boundary value problem (22) provides the average values of the complex fields u^* and θ^* , as well as the average value of λ^* . On the contrary, the solution of the boundary value problem (23) yields the oscillating components of these quantities. Indeed, the values of λ_b^* , θ_b^* and ζ can be determined by employing the constraint equations. For instance, the constraint on $\theta_a^*(r)$ yields $\zeta = 0$, i.e. $T_1 = T_0$. The solution of Eq. (22) is

$$\theta_a^*(r) = 0, \quad u_a^*(r) = 2(1 - 4r^2), \quad \lambda_a^* = 32. \tag{24}$$

As expected, the velocity distribution $u_a^*(r)$ is the well known Poiseuille velocity profile. On the other hand, the dimensionless temperature distribution $\theta_b^*(r)$ which fulfils Eq. (23) is given by

$$\theta_b^*(r) = \frac{I_0(r\sqrt{i\Omega Pr})}{I_0(\sqrt{i\Omega Pr}/2)}. \tag{25}$$

By substituting Eq. (25) into Eq. (23), one obtains the following boundary value problem

$$\frac{1}{r} \frac{d}{dr} \left(r \frac{du_b^*}{dr} \right) - i\Omega u_b^* + \lambda_b^* + \frac{I_0(r\sqrt{i\Omega Pr})}{I_0(\sqrt{i\Omega Pr}/2)} = 0,$$

$$u_b^*(1/2) = 0, \quad \int_0^{1/2} dr u_b^*(r)r = 0. \tag{26}$$

The homogeneous equation associated with the boundary value problem (26) is

$$\frac{d^2 u_b^*}{dr^2} + \frac{1}{r} \frac{du_b^*}{dr} - i\Omega u_b^* = 0. \tag{27}$$

A pair of linearly independent solutions of Eq. (27) is $I_0(r\sqrt{i\Omega})$ and $K_0(r\sqrt{i\Omega})$ [12]. The Wronskian of these solutions is given by

$$W(r) = I_0(r\sqrt{i\Omega}) \frac{dK_0(r\sqrt{i\Omega})}{dr} - K_0(r\sqrt{i\Omega}) \frac{dI_0(r\sqrt{i\Omega})}{dr}. \tag{28}$$

On account of the identity [12]

$$K_0(s) \frac{dI_0(s)}{ds} - I_0(s) \frac{dK_0(s)}{ds} = \frac{1}{s}, \tag{29}$$

one obtains

$$W(r) = -\frac{1}{r}. \tag{30}$$

As a consequence of a theorem on linear differential equations [13], the general solution of the inhomogeneous differential equation in the boundary value problem (26) has the form

$$\begin{aligned} u_b^*(r) = & A_1 I_0(r\sqrt{i\Omega}) + A_2 K_0(r\sqrt{i\Omega}) \\ & + I_0(r\sqrt{i\Omega}) \int_0^r ds K_0(s\sqrt{i\Omega}) sF(s) \\ & - K_0(r\sqrt{i\Omega}) \int_0^r ds I_0(s\sqrt{i\Omega}) sF(s), \end{aligned} \tag{31}$$

where A_1 and A_2 are two integration constants and the function $F(s)$ is given by the inhomogeneous term of the differential equation which appears in Eq. (26), namely

$$F(s) = -\lambda_b^* - \frac{I_0(s\sqrt{i\Omega Pr})}{I_0(\sqrt{i\Omega Pr}/2)}. \tag{32}$$

The integration constant A_2 must be zero, since the velocity distribution must be finite at $r = 0$. On the contrary, the integration constant A_1 can be determined on account of the boundary condition expressed in Eq. (26). One can rewrite Eq. (31) as follows:

$$\begin{aligned} u_b^*(r) = & A_1 I_0(r\sqrt{i\Omega}) + \lambda_b^* [G_3(r, \Omega) - G_1(r, \Omega)] \\ & + G_4(r, \Omega, Pr) - G_2(r, \Omega, Pr), \end{aligned} \tag{33}$$

where the functions G_1, G_2, G_3 and G_4 are defined as:

$$G_1(r, \Omega) = \frac{I_0(r\sqrt{i\Omega})}{i\Omega} \left[1 - r\sqrt{i\Omega} K_1(r\sqrt{i\Omega}) \right],$$

$$\begin{aligned} G_2(r, \Omega, Pr) = & \frac{I_0(r\sqrt{i\Omega})}{i\Omega(1-Pr)I_0(\sqrt{i\Omega Pr}/2)} \\ & \times \left[1 - r\sqrt{i\Omega Pr} \times K_0(r\sqrt{i\Omega}) I_1(r\sqrt{i\Omega Pr}) \right. \\ & \left. - r\sqrt{i\Omega} K_1(r\sqrt{i\Omega}) I_0(r\sqrt{i\Omega Pr}) \right], \end{aligned}$$

$$G_3(r, \Omega) = \frac{r}{\sqrt{i\Omega}} K_0(r\sqrt{i\Omega}) I_1(r\sqrt{i\Omega}),$$

$$\begin{aligned} G_4(r, \Omega, Pr) = & \frac{rK_0(r\sqrt{i\Omega})}{i\Omega(1-Pr)I_0(\sqrt{i\Omega Pr}/2)} \\ & \times \left[\sqrt{i\Omega} I_1(r\sqrt{i\Omega}) I_0(r\sqrt{i\Omega Pr}) \right. \\ & \left. - \sqrt{i\Omega Pr} I_0(r\sqrt{i\Omega}) I_1(r\sqrt{i\Omega Pr}) \right]. \end{aligned} \tag{34}$$

As a consequence of the boundary condition in Eq. (26), the integration constant A_1 is given by

$$\begin{aligned} A_1 = & \lambda_b^* \frac{G_1(1/2, \Omega) - G_3(1/2, \Omega)}{I_0(\sqrt{i\Omega}/2)} \\ & + \frac{G_2(1/2, \Omega, Pr) - G_4(1/2, \Omega, Pr)}{I_0(\sqrt{i\Omega}/2)}. \end{aligned} \tag{35}$$

Moreover, the parameter λ_b^* can be evaluated by utilizing the constraint equation which appears in Eq. (26), namely

$$\begin{aligned} \lambda_b^* = & - \left[G_3(1/2, \Omega) \frac{G_2(1/2, \Omega, Pr) - G_4(1/2, \Omega, Pr)}{I_0(\sqrt{i\Omega}/2) K_0(\sqrt{i\Omega}/2)} \right. \\ & \left. - \int_0^{1/2} dr G_2(r, \Omega, Pr)r + \int_0^{1/2} dr G_4(r, \Omega, Pr)r \right] \\ & \times \left[G_3(1/2, \Omega) \frac{G_1(1/2, \Omega) - G_3(1/2, \Omega)}{I_0(\sqrt{i\Omega}/2) K_0(\sqrt{i\Omega}/2)} \right. \\ & \left. - \int_0^{1/2} dr G_1(r, \Omega)r + \int_0^{1/2} dr G_3(r, \Omega)r \right]^{-1}. \end{aligned} \tag{36}$$

On account of Eqs. (15), (19) and (21), also the Fanning friction factor can be rewritten as follows:

$$fRe = \mathcal{R}e(f_a^* Re + f_b^* Gre^{in}), \tag{37}$$

where f_a^* and f_b^* are respectively given by

$$f_a^* Re = -2 \frac{du_a^*}{dr} \Big|_{r=1/2} = 16 \tag{38}$$

and

$$f_b^* Re = -2 \frac{du_b^*}{dr} \Big|_{r=1/2} \quad (39)$$

Finally, a dimensionless heat flux can be defined as

$$\Phi = \frac{2R_0 q}{k\Delta T} = \frac{\partial \theta}{\partial r} = \mathcal{R}e \left(\frac{\partial \theta^*}{\partial r} \right) = \mathcal{R}e(\Phi^*) \quad (40)$$

As a consequence of Eqs. (21), (24) and (25), the complex valued function $\Phi^* = \partial \theta^* / \partial r$ can be expressed as

$$\Phi^* = \Phi_a^* + \Phi_b^* e^{i\eta}, \quad (41)$$

where $\Phi_a^* = 0$ and

$$\Phi_b^* = \frac{\partial \theta_b^*}{\partial r} = \frac{\sqrt{i\Omega Pr} I_1(r\sqrt{i\Omega Pr})}{I_0(\sqrt{i\Omega Pr}/2)} \quad (42)$$

4. Discussion of the results

In this section, a survey of the solution obtained above is performed by representing the radial distributions of the oscillation amplitudes of the dimensionless temperature as well as of the dimensionless velocity, for fixed values of the parameters Gr/Re , Ω , and Pr . Moreover, the influence of the dimensionless parameters Ω and Pr on the oscillation amplitudes of λ and of fRe is analyzed.

In Fig. 1, the dimensionless temperature distribution $|\theta_b^*|$ is reported versus the dimensionless radius r , for different values assumed by the product ΩPr . This figure shows that $|\theta_b^*|$ is a monotonic increasing function of r and that, for increasing values of ΩPr , the oscillations of the dimensionless temperature tend to be confined in a narrow region close to the duct wall.

Figs. 2–5 represent the radial distribution of $|u_b^*|$, for fixed values of the parameter Pr and for different values

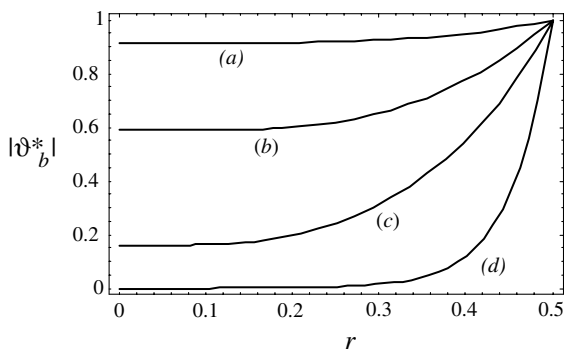


Fig. 1. Radial distribution of $|\theta_b^*|$ for $\Omega Pr = 10$ (a), $\Omega Pr = 30$ (b), $\Omega Pr = 100$ (c) and $\Omega Pr = 1000$ (d).

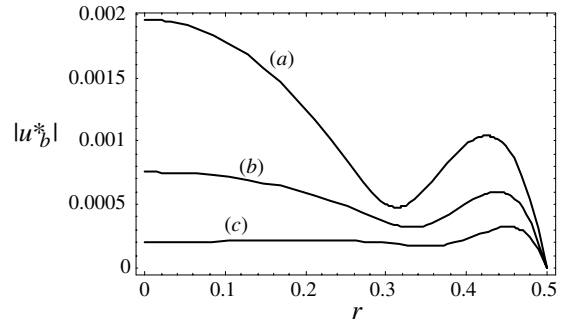


Fig. 2. Radial distribution of $|u_b^*|$ for $Pr = 7$ and for $\Omega = 50$ (a), $\Omega = 100$ (b) and $\Omega = 200$ (c).

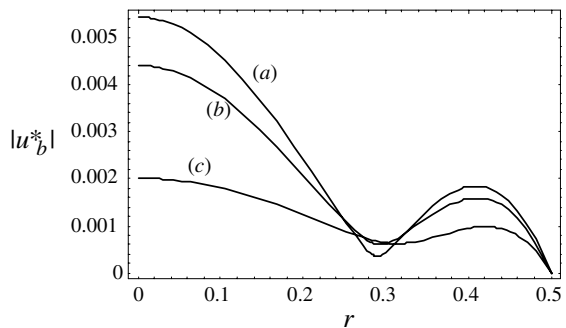


Fig. 3. Radial distribution of $|u_b^*|$ for $Pr = 0.7$ and for $\Omega = 50$ (a), $\Omega = 100$ (b) and $\Omega = 200$ (c).

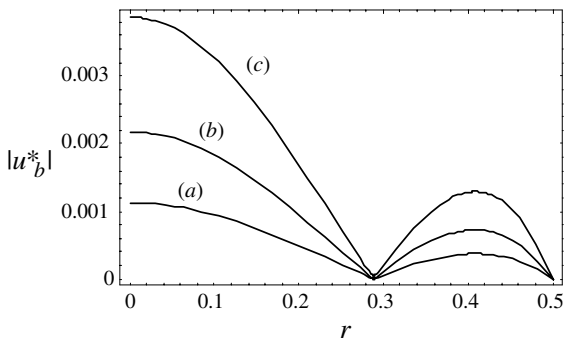


Fig. 4. Radial distribution of $|u_b^*|$ for $Pr = 7$ and for $\Omega = 0.5$ (a), $\Omega = 1$ (b) and $\Omega = 2$ (c).

assumed by the parameter Ω . In particular, Figs. 2 and 4 refer to $Pr = 7$ while Figs. 3 and 5 refer to $Pr = 0.7$. These figures show that $|u_b^*|$ has two local maxima, one placed on the duct axis and the other close to the duct wall. Moreover, in Figs. 2–5 the presence of a local minimum arises for $r \approx 0.3$. This local minimum is more

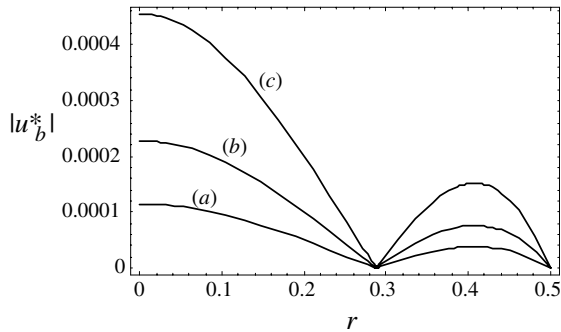


Fig. 5. Radial distribution of $|u_b^*|$ for $Pr = 0.7$ and for $\Omega = 0.5$ (a), $\Omega = 1$ (b) and $\Omega = 2$ (c).

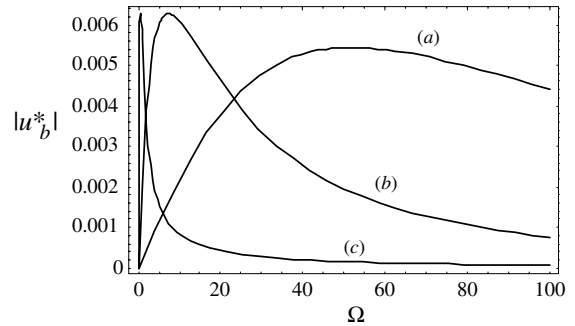


Fig. 6. Distribution of $|u_b^*|$ versus Ω , for $r = 0$ and $Pr = 0.7$ (a), $Pr = 7$ (b) and $Pr = 100$ (c).

evident in Figs. 4 and 5, which refer to lower values of the dimensionless frequency Ω ($\Omega \leq 2$).

Moreover, for any radial position there exists a dimensionless resonance frequency such that the oscillation amplitude of the dimensionless velocity distribution reaches a maximum. This resonance frequency is a function of the radial position and of the Prandtl number. The phenomenon is evident in Figs. 6 and 7, where the dimensionless velocity distribution is reported versus the dimensionless frequency, for fixed values of the radial coordinate and of the parameter Pr . In Table 1, the values of the resonance frequency are reported for different values of the parameter Pr and of the dimensionless radial position. This Table shows that, for any value of Pr , the resonance frequency is not a monotonic function of r . In particular, the resonance frequency reaches a relative maximum for $r \approx 0.3$, which approximately correspond to the radial position in which $|u_b^*|$ has a local minimum.

In Fig. 8, the oscillation amplitude of the dimensionless pressure drop is reported versus the dimensionless frequency Ω , for some values assumed by the parameter Pr . This Figure shows that $|\lambda_b^*|$ is a monotonic decreasing function of Ω and that it decreases more rapidly when the Prandtl number assumes higher values.

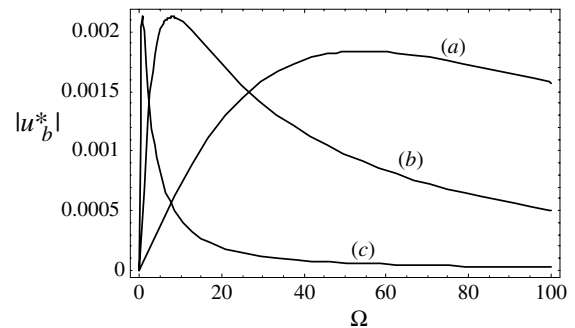


Fig. 7. Distribution of $|u_b^*|$ versus Ω , for $r = 0.4$ and $Pr = 0.7$ (a), $Pr = 7$ (b) and $Pr = 100$ (c).

In Fig. 9 the oscillation amplitude of the friction factor is reported versus the dimensionless frequency Ω , for different values assumed by Pr . This Fig. 9 shows that, for any value assumed by the Prandtl number, there exists a resonance frequency which maximizes the oscillation amplitude of the friction factor. In Table 2, those resonance frequencies are reported for $0.01 \leq Pr \leq 1000$. The table shows that the resonance frequency is a monotonic decreasing function of the Prandtl number.

Table 1
Dimensionless resonance frequencies of u for different values of the parameter Pr

r	$Pr = 0.01$	$Pr = 0.1$	$Pr = 0.7$	$Pr = 7$	$Pr = 20$	$Pr = 100$
0	255.5	138.8	51.99	7.349	2.582	0.5160
0.05	274.0	140.2	52.06	7.372	2.592	0.5180
0.1	352.3	145.0	52.31	7.449	2.623	0.5246
0.15	458.2	155.2	52.92	7.609	2.687	0.5382
0.2	565.2	178.0	54.70	7.991	2.837	0.5695
0.25	721.5	240.5	70.48	10.72	3.851	0.7765
0.3	935.0	334.0	147.8	28.20	8.959	1.668
0.35	294.9	159.0	55.58	7.684	2.682	0.5343
0.4	612.1	180.1	54.52	7.949	2.820	0.5659
0.45	1226	214.2	55.73	8.360	2.999	0.6047

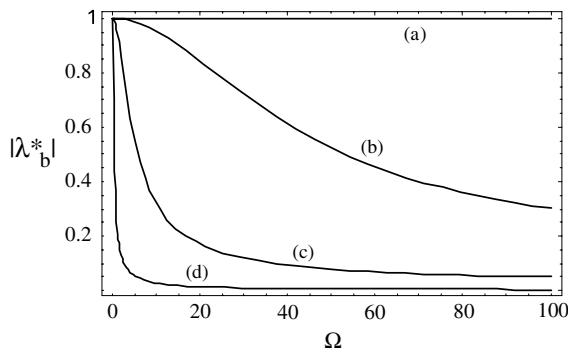


Fig. 8. Distribution of $|\lambda_b^*|$ versus Ω , for $Pr = 0.01$ (a), $Pr = 0.7$ (b), $Pr = 7$ (c) and $Pr = 100$ (d).

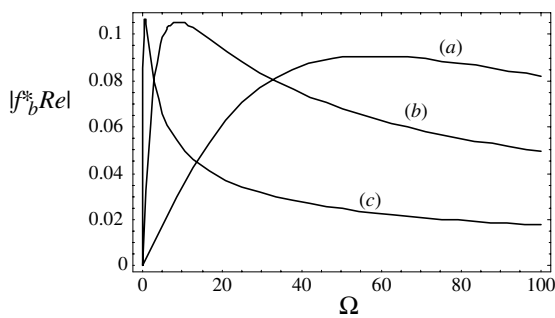


Fig. 9. Distribution of $|f_b^* Re|$ versus Ω , for $Pr = 0.7$ (a), $Pr = 7$ (b) and $Pr = 100$ (c).

Table 2
Dimensionless resonance frequencies of fRe for different values of Pr

Pr	Ω	Pr	Ω
0.01	2462	5	12.20
0.02	1249	10	6.354
0.05	514.3	20	3.237
0.1	266.2	50	1.309
0.2	142.9	100	0.6565
0.5	72.99	200	0.3288
1	45.28	500	0.1316
2	26.87	1000	0.06584

For any radial position, also the oscillation amplitude of the dimensionless heat flux displays a maximum in correspondence of a particular value of the product ΩPr . These resonance values of ΩPr are reported in Table 3. Finally, in Fig. 10 the oscillation amplitude of the dimensionless heat flux is reported versus the dimensionless radial coordinate for different values assumed by the product ΩPr . The figure shows that $|\Phi_b^*|$ is a monotonic increasing function of r .

Table 3
Values of the product ΩPr which correspond to resonances of Φ

r	ΩPr	r	ΩPr
0	49.23	0.275	56.73
0.05	49.23	0.3	61.50
0.075	49.26	0.325	70.60
0.1	49.33	0.35	92.48
0.125	49.48	0.375	143.7
0.15	49.75	0.4	223.0
0.175	50.21	0.425	384.4
0.2	50.95	0.45	842.4
0.225	52.10	0.475	3282
0.25	53.89	0.495	80 400

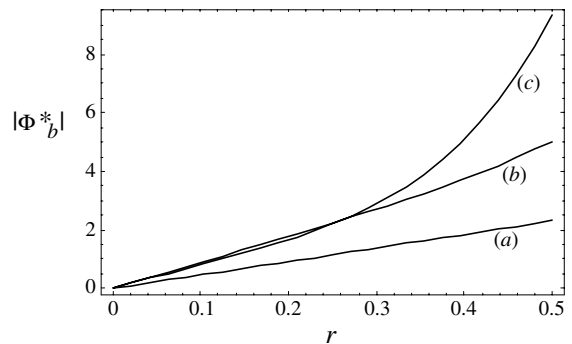


Fig. 10. Distribution of $|\Phi_b^*|$ versus r , for $\Omega Pr = 10$ (a), $\Omega Pr = 30$ (b) and $\Omega Pr = 100$ (c).

5. Conclusions

An analysis of the fully developed laminar mixed convection of a Newtonian fluid in a vertical cylindrical duct with circular cross section has been performed. Reference has been made to the steady periodic regime, by assuming as thermal boundary condition that the wall temperature distribution is a sinusoidal function of time. The velocity and temperature fields, as well as the pressure drop, have been written in a dimensionless form and expressed as real parts of complex valued functions. Thus, two independent boundary value problems have been obtained and solved analytically. The first one accounts for the mean component of each physical quantity, while the second one provides the oscillating component. The dimensionless velocity and temperature have been obtained as functions of three different parameters: the dimensionless frequency Ω , the Prandtl number Pr and the ratio between the Grashof number and the Reynolds number Gr/Re . The oscillating components of the velocity and temperature distributions obtained by the second boundary value problem have been reported versus the dimensionless radial coordinate, for some values of Ω and Pr . Moreover, the

oscillating component of the pressure drop has been reported versus the dimensionless angular frequency Ω . It has been also shown that there exists a resonance frequency such that the velocity oscillations reach a maximum. This resonance frequency depends on the value assumed by Pr and on the radial position.

Finally, the Fanning friction factor and the dimensionless heat flux have been expressed as the sum of a mean component and an oscillating component and evaluated analytically. It has been shown that there exists a resonance frequency which maximizes the amplitude of the friction factor and that this frequency is a monotonic decreasing function of Pr . Finally, it has been shown that there also exists a resonance frequency for the dimensionless heat flux, which is a function of the dimensionless radial position and of the product ΩPr .

References

- [1] E.M. Sparrow, F.M. de Farias, Unsteady heat transfer in ducts with time varying inlet temperature and participating walls, *Int. J. Heat Mass Transfer* 11 (1968) 837–853.
- [2] R.M. Cotta, M.D. Mikhailov, M.-N. Ozišić, Transient conjugated forced convection in ducts with periodically varying inlet temperature, *Int. J. Heat Mass Transfer* 30 (1987) 2073–2082.
- [3] K.N. Krishnan, V.M.K. Sastri, Heat transfer in laminar pulsating flows of fluids with temperature dependent viscosities, *Wärme Stoffübertrag.* 24 (1989) 37–42.
- [4] K. Mansouri, B. Fourcher, Réponse à un signal thermique sinusoidal dans le cas d'un écoulement laminaire à plan directeur, *Int. Commun. Heat Mass Transfer* 22 (1995) 305–315.
- [5] D.-Y. Lee, S.-J. Park, S.T. Ro, Heat transfer by oscillating flow in a circular pipe with sinusoidal wall temperature distribution, *Int. J. Heat Mass Transfer* 38 (1995) 2529–2537.
- [6] M. Kazmierczak, Z. Chioda, Buoyancy-driven flow in an enclosure with time periodic boundary conditions, *Int. J. Heat Mass Transfer* 35 (1992) 1507–1518.
- [7] H.S. Kwak, K. Kuwahara, J.M. Hyun, Resonant enhancement of natural convection heat transfer in a square enclosure, *Int. J. Heat Mass Transfer* 41 (1998) 2837–2846.
- [8] J.L. Lage, A. Bejan, The resonance of natural convection in an enclosure heated periodically from the side, *Int. J. Heat Mass Transfer* 36 (1993) 2027–2038.
- [9] B.V. Antohe, J.L. Lage, Amplitude effect on convection induced by time periodic horizontal heating, *Int. J. Heat Mass Transfer* 39 (1996) 1121–1133.
- [10] U.N. Das, R.K. Deka, V.M. Soundalgekar, Transient free convection flow past an infinite vertical plate with periodic temperature variation, *ASME J. Heat Transfer* 121 (1999) 1091–1094.
- [11] A. Barletta, E. Zanchini, Time-periodic laminar mixed convection in an inclined channel, *Int. J. Heat Mass Transfer* 46 (2003) 551–563.
- [12] S. Gradshteyn, I.M. Ryzhik, *Table of Integrals Series and Products*, Academic Press, New York, NY, 1965.
- [13] C.R. Wylie, *Advanced Engineering Mathematics*, McGraw-Hill, New York, NY, 1960, pp. 99–101.